Numerical analysis of focusing by a metamaterial lens

Ali Eren Culhaoglu[1], **Andrey Osipov**[1] **and Peter Russer**[2]

[1] Microwaves and Radar Institute, German Aerospace Center
82234 Wessling Germany
email: Ali.Culhaoglu@dlr.de

[2] Institute for High Frequency Engineering, Technische Universität München
Arcisstrasse 21, 80333 Munich Germany
email: russer@tum.de

Abstract Over the last several years there has been a surge of interest in artificial materials because of their potential to expand the range of electromagnetic properties in materials. The so called metamaterials, also known as left-handed (LHM) or double-negative (DNG) materials with negative permittivity and permeability have attracted growing interest. An important application area is the realization of flat superlenses with imaging properties beyond that of conventional lenses. This work investigates the focusing properties of a lossless planar DNG slab with a relative permittivity and permeability both approaching the value -1. The relation between the imaging quality and the material parameters is examined both analytically and numerically. Results obtained from numerical simulations via the transmission line matrix method are compared to the analytical solution.

1. Introduction

Incident and emerging waves from a DNG slab will undergo negative refraction [1]. As a consequence a slab with finite thickness d and material parameters ε_r = μ_r = -1 (refractive index $n = \sqrt{\varepsilon_r \mu_r}$ = -1) focuses waves emitted from a point source located at a distance l in front of the slab to a point at a distance of $d - l$ behind the slab [2, 3]. As seen in Fig. 1(a) the waves emitted from a point source are focused inside and outside the slab due to negative refraction at the slab interfaces. Furthermore modes with large wavenumbers excite surface waves along the slab interfaces restoring the evanescent field which decays exponentially away from the source [4]. Therefore a transversely unbounded slab is capable of focusing every mode of the emitted spectrum from a point source reproducing a perfect image. On the contrary the focusing quality in a conventional lens is largely determined by its curvature and aperture size which results in a diffraction limited pattern [5]. The impact of the lateral extension of a finite sized DNG slab (i.e. having finite aperture) onto its imaging quality has already been investigated numerically in [6]. As it will be shown in the following sections, the electromagnetic field behavior at the image plane is largely determined by resonant peaks occuring in the transmission coefficient of the slab. The effect of the deviation from the ideal material parameters of ε_r = μ_r = -1 onto the imaging quality will be investigated by the method described in [7]. Thereby a slight perturbation σ is applied to ε_r and μ_r whilst retaining the refractive index of $n = -1$ and considering the problem in the limiting case as $\sigma \to 0$. Finally numerical simulations, based on the modified transmission line matrix (TLM) scheme are carried out and the results are compared to the analytical solution.

2. Analytical Solution

We consider the setup given in Fig. 1(a). Since the configuration is unbounded in the transversal direction circular-cylindrical coordinates (ρ, z) will be used. A hertzian dipole

$$J(\rho, z) = I_0 \delta(\rho)\delta(z - z')\hat{\mathbf{z}} \tag{1}$$

is placed on the z-axis at z' = $z_0 < 0$ in front of a DNG slab with refractive index $n = -\sqrt{\varepsilon_r \mu_r}$ and thickness d. The impedances and spectral wavenumbers along the optical axis (**z**-axis) are

$$k_z^{air} = \sqrt{k_0^2 - k_t^2} \quad \text{and} \quad Z_0 = \frac{k_z^{air}}{\omega \epsilon_0}, \tag{2}$$

in free space and

$$k_z^{slab} = \sqrt{n^2 k_0^2 - k_t^2} \quad \text{and} \quad Z = \frac{k_z^{slab}}{\omega \epsilon_r} \tag{3}$$

inside the slab, where $k_t = \sqrt{k_\phi^2 + k_\rho^2}$ is the transversal wave number parallel to the plane of the slab interface. The resulting electromagnetic fields behind the slab $z > d$, for a time dependence of e^{-iwt}, are given as [8, 9]

$$\boldsymbol{E}(\rho, z) = \frac{-I_0}{8\pi\omega\epsilon_0} \nabla \times \nabla \times \int_{\infty_{e^{i\pi}}}^{\infty} \frac{k_t}{k_z^{air}} H_0^{(1)}(k_t \rho) e^{ik_z^{air}(z-d+|z_0|)} T(k_t) dk_t \tag{4}$$

$$\boldsymbol{H}(\rho, z) = \frac{iI_0}{8\pi} \nabla \times \int_{\infty_{e^{i\pi}}}^{\infty} \frac{k_t}{k_z^{air}} H_0^{(1)}(k_t \rho) e^{ik_z^{air}(z-d+|z_0|)} T(k_t) dk_t. \tag{5}$$

$T(k_t)$ being the transmission coefficient of the slab and is defined as

$$T(k_t) = \frac{1}{\cos(k_z^{slab} d) - \frac{i}{2}\sin(k_z^{slab} d)(\frac{Z}{Z_0} + \frac{Z_0}{Z})}. \tag{6}$$

The integration is over the entire spectrum containing both propagating ($k_t < k_0$) and evanescent ($k_t > k_0$) modes. For the perfect imaging condition ε_r = μ_r = -1 the integrals in (4) and (5) simplify to

$$\int_{\infty_{e^{i\pi}}}^{\infty} \frac{k_t}{\tilde{k}} H_0^{(1)}(k_t \rho) e^{i\tilde{k}(z-2d+|z_0|)} dk_t \tag{7}$$

where $\tilde{k} = k_z^{air} = k_z^{slab}$. The integration is performed in closed form (equation 6.616 - 3 in [10]) and the result is

$$\boldsymbol{E}(\rho, z) = \frac{iI_0}{4\pi\omega\epsilon(z)} \nabla \times \nabla \times \frac{e^{ik_0\sqrt{\rho^2 + (z-2d+|z_0|)^2}}}{\sqrt{\rho^2 + (z - 2d + |z_0|)^2}} \tag{8}$$

and

$$\boldsymbol{H}(\rho, z) = \frac{I_0}{4\pi} \nabla \times \frac{e^{ik_0\sqrt{\rho^2 + (z-2d+|z_0|)^2}}}{\sqrt{\rho^2 + (z - 2d + |z_0|)^2}}, \tag{9}$$

which are identical to that of a dipole situated at $z = 2d - |z_0|$. Therefore it is evident that a perfect reproduction of the source is obtained. In order to investigate the sensitivity of the imaging quality to the material parameters they are perturbed from their ideal values of ε_r = μ_r = -1 by σ according to

$$\varepsilon_r = -(1+\sigma) \quad \text{and} \quad \mu_r = -\frac{1}{1+\sigma}. \tag{10}$$

The refractive index remains thereby unchanged and retains its value of $n = -1$. The impedance is no more unity and becomes $\sqrt{\frac{\mu_r}{\epsilon_r}} = \frac{1}{1+\sigma}$. Note that as $\sigma \to 0$ the impedance of the slab will be unity and therefore perfectly matched to free space. Substituting these parameters into the integrals (4) and(5) results in the following expression

$$-\int_{\infty_{e^{i\pi}}}^{\infty} \frac{k_t H_0^{(1)}(k_t\rho)2(1+\sigma)e^{i\tilde{k}(z-d+|z_0|)}}{\tilde{k}(-2\cos(\tilde{k}d) - 2\cos(\tilde{k}d)\sigma + 2i\sin(\tilde{k}d) + 2i\sin(\tilde{k}d)\sigma + i\sin(\tilde{k}d)\sigma^2)} dk_t \tag{11}$$

with an additional pole at the critical wavenumber

$$k_c = \pm k_0 \sqrt{1 + \left[\frac{1}{k_0 d}\tanh^{-1}\left(\frac{2+2\sigma}{2+2\sigma+\sigma^2}\right)\right]^2}. \tag{12}$$

The integral can now be evaluated numerically along the contour shown in Fig. 1(b). The wavenumber k_c is associated with the excitation of surface waves and has a strong effect onto the minimum resolvable feature by the slab. The resolution enhancement is dependent on the value of k_c and can be given as the ratio of k_c/k_0 [11]. Note that the main contribution to the integral (11) comes from that part of the spectrum determined by resonant peaks occuring in the transmission coefficient of the slab. As $\sigma \to 0$ $k_c \to \infty$ and the ideal case of ε_r = μ_r=-1 with a perfect resolution will be achieved.

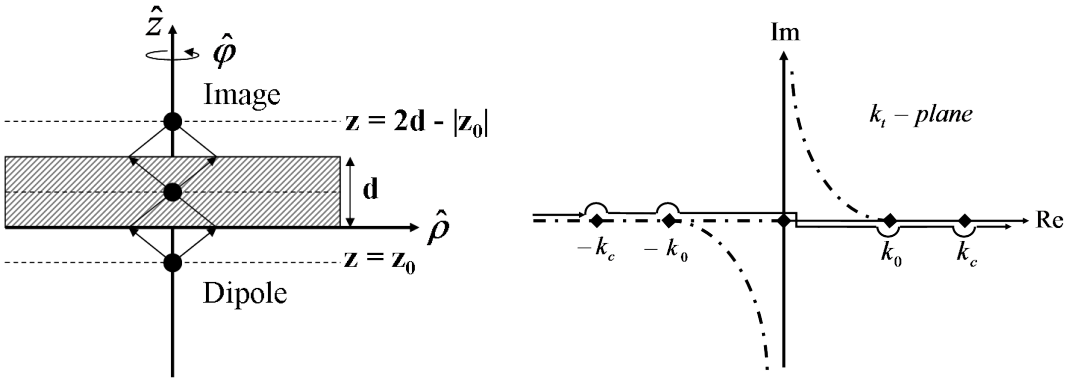

(a) (b)

Fig. 1: (a) Focusing property of a metamaterial slab of thickness d, with a point source placed at $z = z_0$ (b) Contour of integration. The path is deformed into small semicircles at the poles.

3. Numerical Simulations

The modified transmission line matrix (TLM) scheme yields a general framework for the modeling of a composite right left handed (CRLH) metamaterial. The simulations have been carried out with MEFISTo-3D Pro, a full wave time domain electromagnetic simulation tool based on the TLM method. Negative refractive index materials are modeled by matching an inter cell network to a standard 3D SCN node. As explained in [12] the discretization of the structure plays thereby an important role and the cell

size Δl should be much smaller than the operating wavelength ($\Delta l/\lambda << 1$). In this work we consider a lossless and impedance matched (to free space) CRLH slab with $\varepsilon_r = \mu_r = -1$ at a design frequency of f= 5 GHz. A dipole oscilatting at 5 GHz is placed at distance of $\lambda/4$ in front of the slab whose thickness is varied between $\lambda/3 < d < 2\lambda$. The simulation region has dimensions of 10λ x 10λ and is terminated by a perfectly matched absorbing boundary layer condition (Fig. 2). The spatial step size is $\lambda/60$. All simulations have been truncated at $t = 4000\Delta t$, where a steady state has been reached. Field monitors are placed along the expected image plane at a distance of $d - \lambda/4$ behind the slab and the intensity distribution is calculated by computing the time averaged electric field intensities. The spot size R which gives a measure for the focusing quality is defined as the full width at half maximum (FWHM) value of the main lobe of the intensity pattern

$$R = \frac{\Delta\rho}{\lambda} \tag{13}$$

with $\Delta\rho = \rho_{I_{max}} - \rho_{I_{max}/2}$ being the distance over which the intensity falls to half its maximum value along the image plane. The enhancement in resolution is then given by R^{-1}.

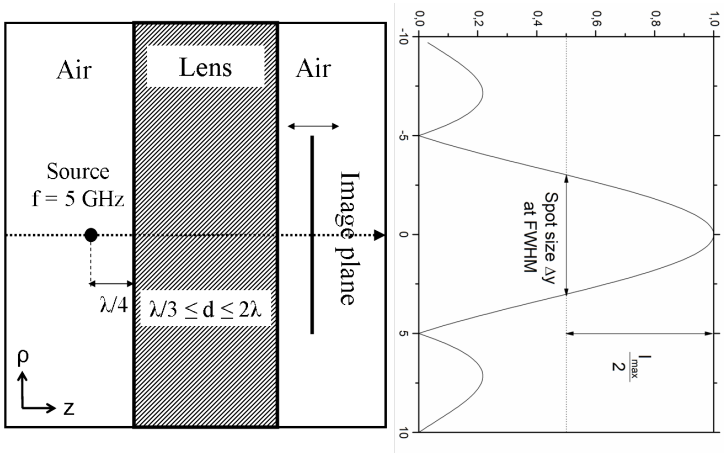

Fig. 2: Simulation space and expected intensity distribution along image plane.

4. Results

For a perfect image the spot size defined in (13) should become infinitesimally small as $\sigma \to 0$ resulting in an arbitrarily fine resolution $R^{-1} = \infty$. Therefore it is expected that $\Delta\rho$ gets smaller as $\sigma \to 0$. Fig. 3(a) shows the intensity patterns along the image plane for a slab of thickness $d = \lambda/2$ and various values of σ obtained from the analytical model by integrating (11) numerically. The intensity pattern is normalized with respect to the the maximum intensity at $\rho = 0$. As expected the width of the main lobe narrows as $\sigma \to 0$ which indicates an enhancement in the resolution. A direct comparison between the numerical and analytical results reveals that the simulation results correspond to the analytical model with a perturbation factor of $\sigma = 0.1$ and a resolution enhancement of $R^{-1} = 4$. The DNG medium model is implemented in MEFISTo-3D Pro by a matching network. As explained in [12] the discretization of the structure plays thereby an important role and the cell size Δl should be much smaller than the operating wavelength ($\Delta l/\lambda << 1$). Throughout the simulations a discretization of 1 mm was used which corresponds to $\lambda/60$. Therefore it is expected that the simulated resolution will enhance by discretizing the structure with a finer mesh. The resolution enhancement R^{-1} obtained from the analytical model as a function of σ is plotted in Fig. 3(c). As $\sigma \to 0$ the resolution increases in accordance with the wavenumber given in (12), which varies for small values of σ as $\ln\sigma$. On the other hand for larger

perturbation values it can be seen that the resolution degrades significantly. Furthermore the impact of the slab thickness on the focusing quality has been investigated. The thickness of the slab is varied between $\lambda/3$ and 2λ, while the point source is held fixed at a distance of $\lambda/4$ from the slab. The results are plotted in Fig. 3(b). It is observed that the focusing quality degrades with incresing slab thickness. From Fig. 3(d) it can be seen that the improvement in the resolution is very significant for thin slabs . A further increase of the slab thickness, beyond a thickness to wavelength ratio of approximately $d/\lambda = 1$ results only in a small enhancement of the resolution.

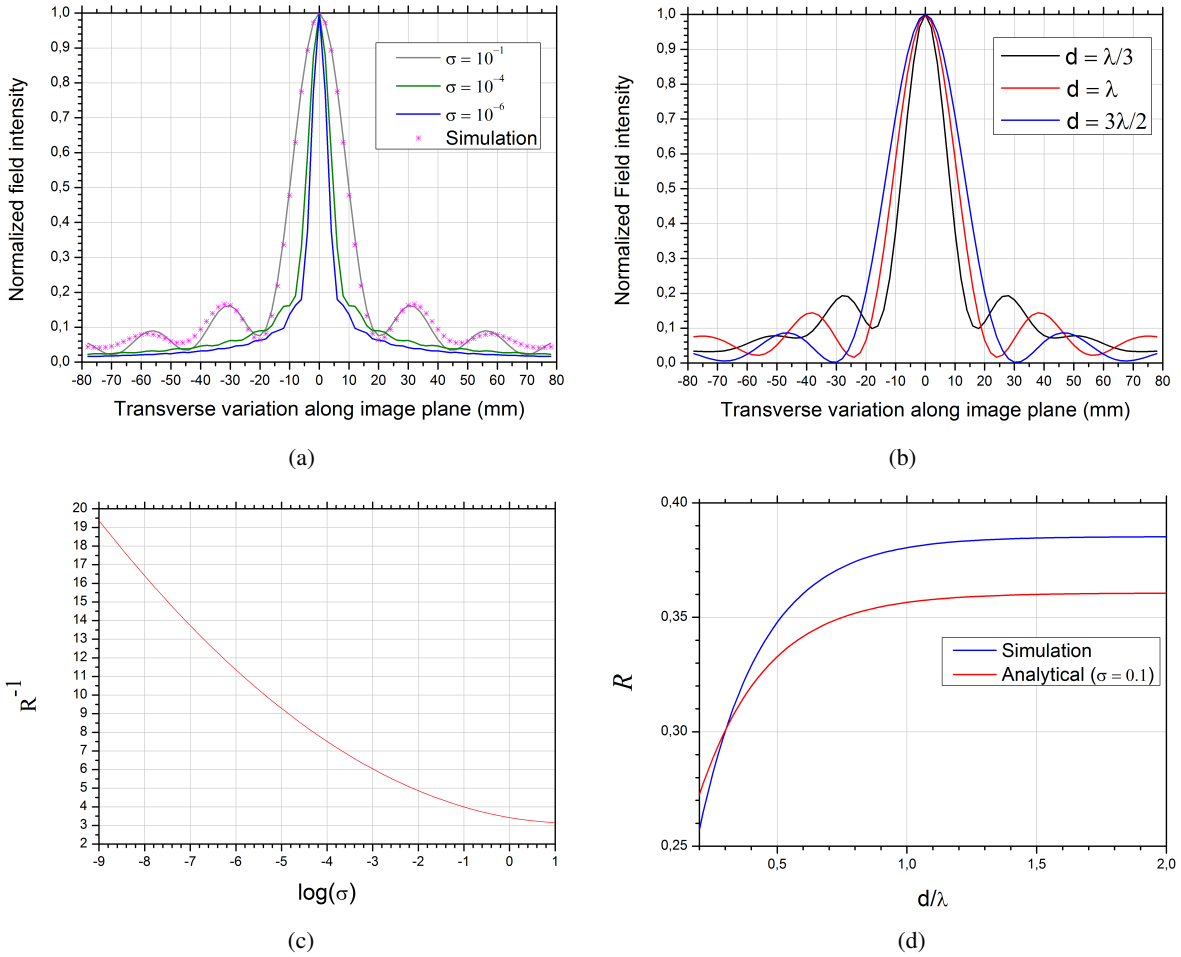

Fig. 3: (a) Comparison of intensity distribution along image plane obtained from the analytical model (by integrating (11)) for various perturbation values and MEFISTo simulation results ($d = \lambda/2$, $z_0 = -\lambda/4$, f= 5 GHz) (b) MEFISTo simulation results. Intensity distribution along image plane for varying slab thicknesses ($\lambda/3 < d < \lambda$). The source is held fixed at $z_0 = -\lambda/4$ and the position of the image plane adjusted according to the slab thickness (c) Resolution enhancement as a function of $\log \sigma$ obtained by integrating (11) (d) Effect of slab thickness on resolution.

5. Conclusion

The focusing property of a 2D metamaterial slab was studied both analytically and numerically. The analysis was carried out through a perturbation of the material parameters from their ideal values of $\varepsilon_r = \mu_r = -1$, for which $k_c \to \pm\infty$. Thereby it was shown that the resolution enhancement depends primarily on the extent by which the surface waves are excited. The main contribution to the integral

in (11) comes from the part of the evanescent spectrum close to the wavenumber by which surface waves are excited at the interfaces of the slab. Small deviations from the ideal material parameters result in a significant loss of the focusing quality. The accuracy of the numerical calculations are strongly dependent on the discretization and are valid for electrically short transmission lines with $\Delta l/\lambda << 1$. Therefore it is difficult to simulate a perfect image in which case a very fine meshing is required. However subwavelength imaging with a resolution enhancement of $R^{-1} = 4$ was achieved. To sum up the perfect imaging phenomena is very sensitive to the material parameters and even a small deviation from them will result in a significant degradation of the imaging quality.

References

[1] V. G. Veselago, The Electrodynamics of Substances with Simultaneously Negative Values of ϵ and μ, *Sov. Phys. Uspekhi*, Vol. 10, pp. 509, 1968.

[2] J. B. Pendry, Negative Refraction Makes a Perfect Lens, *Phys. Rev. Lett.,* vol. 85, no. 18, pp. 2933, 2000.

[3] A. Grbic and G. V. Eleftheriades, Overcoming the Diffraction Limit with a Planar Left-Handed Transmission-Line Lens, *Phys. Rev. Lett. ,* vol. 92, no. 11, 2004.

[4] Nicholas Fang and Xiang Zhang, Imaging properties of a metamaterial superlens, *Appl. Phys. Lett.,* vol. 82, no. 2, pp. 161, 2003.

[5] E. Born and Emil Wolf, Principles of Optics: Electromagnetic Theory of Propagation, Interference and Diffraction of Light, *Cambridge Univ. Pr.,* 1999.

[6] Ali Eren Culhaoglu, Michael Zedler, Wolfgang J. R. Hoefer, Andrey Osipov and Peter Russer, Full Wave Numerical Simulation of a Finite 3D Metamaterial Lens, *Conference Proceedings ACES 2008*, Niagra Falls Canada.

[7] O. E. French, K. I. Hopcraft and E Jakeman, Perturbation on the perfect lens: the near perfect lens, *New Journal of Physics,* vol. 8, no. 8, pp. 271, 2006.

[8] L. B. Felsen and N. Marcuvitz, Radiation and scattering of waves, *IEEE Press,* 1994.

[9] R. W. Ziolkowski and Ehud Heyman, Wave Propagation in Media Having Negative Permittivity and Permeability, *Phys. Rev. E,* vol. 64, no. 056635, 2001.

[10] I.S. Gradshteyn and I.M. Ryzhik, Table of Integrals Series and Products, 7th Edition, Elsevier Academic Press, 2007.

[11] D. R. Smith, D. Schurig, M. Rosenbluth, S. Schultz, S. A. Ramakrishna and J. Pendry, Limitations on Subdiffraction Imaging With a Negative Refractive Index Slab, *Appl. Phys. Lett.,* vol. 82, no. 10, pp. 1506, 2003.

[12] Poman P. M. So, Huilian Du and W. J. R. Hoefer, Modeling of Metamaterials with Negative Refractive Index Using 2-D Shunt and 3D- SCN TLM Networks, *IEEE Trans. on Microwave Theory and Techniques,* vol. 53, no. 4, pp. 9480, 2005.